Journal of Electroceramics, 14, 139–148, 2005

Dielectric Properties of Niobium and Lanthanum Doped Lead Barium Zirconate Titanate Relaxor Ferroelectrics

MING-JEN PAN,[1,*] ROY J. RAYNE[2] & BARRY A. BENDER[2]

[1] *Nova Research, Inc., c/o Code 6350, Naval Research Laboratory, 4555 Overlook Avenue SW, Washington, DC 20375*
[2] *Code 6350, Naval Research Laboratory, 4555 Overlook Avenue SW, Washington, DC 20375*

Submitted April 13, 2004; Revised August 27, 2004; Accepted August 31, 2004

Abstract. The lead barium zirconate titanate (PBZT) relaxor ferroelectrics are ideal for high voltage capacitor applications due to their high dielectric constant, stability under DC bias, and temperature stability. In this study the composition $(Pb_{0.65}Ba_{0.35})(Zr_{0.70}Ti_{0.30})O_3$ was selected as the base composition. It exhibited typical relaxor characteristics such as frequency dispersion and diffuse phase transition. The dielectric constant is ∼6000 at room temperature and remains almost constant under electric field as high as 20 kV/cm. To further enhance the dielectric properties, various amounts of niobium oxide and lanthanum oxide dopants were added to the base PBZT to alter the defect structure and hence the dielectric properties. It was found that the dielectric constant of 1% Nb-doped samples was increased by 20–25% while maintaining similar voltage stability. This increase was attributed to the abnormal grain growth in the Nb-doped sample, and the correlation between microstructure and dielectric constant was drawn through a grain size study. The La addition only caused a monotonic decrease of dielectric constant and slightly improved voltage stability.

Keywords: dielectric properties, relaxor ferroelectrics, DC bias effect, grain size effect

Introduction

In the past decade, the power electronics industry has made tremendous progress in the performance of semiconductor switches in terms of switching speed and efficiency. In contrast, the passive components, especially capacitors, have made only marginal improvement and remained a limiting factor in power converter design. The low stored energy density of current capacitors is a major issue for shipboard services—in a typical state-of-the-art power converter, filter capacitors can take up more than half of the overall volume. As an integral part of the Navy's power electronics effort, our goal is to develop a ceramic dielectric material that is suitable for the high voltage DC link capacitor application, which requires not only high dielectric constant, but also stability under DC bias electric field.

*Corresponding author. E-mail: pan@anvil.nrl.navy.mil

Most commercially available ceramic dielectrics are not suitable for high voltage DC link capacitor applications as their dielectric properties are highly dependent on voltage. A good example is barium titanate and modified barium titanate compositions, which have been the workhorse in the multilayer ceramic capacitor industry. When subjected to a high voltage, the dielectric constant of barium titanate decreases dramatically with increasing voltage [1, 2]. To develop a dielectric material that is independent of the DC bias conditions, we chose a lead barium zirconate titanate (PBZT) relaxor composition as the candidate material based on several previous studies on this family of materials [3–6]. In this study, we first focused on the development of a reproducible process so that the final dielectric could be easily transitioned to a capacitor manufacturer. After the processing procedure was established, we shifted our focus to the improvement of PBZT dielectric properties. Specifically, we examined the effects of aliovalent dopants Nb^{5+} and

La^{3+} on the dielectric properties of the PBZT composition with the goal of optimizing PBZT's dielectric constant and stability under DC bias electric field. The donor dopants Nb^{5+} and La^{3+} were expected to reduce the formation of oxygen vacancies and therefore reduce the concentration of domain-stabilizing defect pairs. Similar effects of donor dopants have been observed in lead zirconate titanate [7]. The reduced oxygen vacancy concentration also could lead to improved reliability, as oxygen vacancy migration is considered the major cause of degradation in perovskites.

Experimental Procedure

The base composition $(Pb_{0.65}Ba_{0.35})(Zr_{0.70}Ti_{0.30})O_3$ was selected based on data reported by Furukawa et al. [5]. The composition was prepared by conventional solid state reaction using reagent grade raw powders: PbO (purity 99.9%), $BaCO_3$ (99.8%), ZrO_2 (99.5%, Hf $<$ 100 ppm), and TiO_2 (99.5%), all of which were obtained from Alfa Aesar (Ward Hill, MA). The powders were weighed and then mixed with deionized water, a dispersant (Tamol 901, Rohm and Haas, Philadelphia, PA) and a surfactant (Triton CF-10, Rohm and Haas, Philadelphia, PA) to make a slurry that has a 20 vol% solids loading. After the zirconia milling media was added, the slurry was attrition-milled for 2 hours. The dried power was calcined in an alumina dish at 850°C for 2 hours. The calcined powder was attrition-milled again and then examined by X-ray diffraction (XRD) to ensure phase purity. The particle size distribution of the powder was measured by using a particle size analyzer (CAPA 700, Horiba Instruments Inc., Irvine, CA). The calcined powder was uniaxially pressed into pellets. The pellets were sintered at 1280°C for 2 hours in a lead-rich environment to suppress lead volatilization. Typical weight loss during sintering was 1–2 wt%.

For the dopant study, niobium oxide (Nb_2O_5) and lanthanum oxide (La_2O_3) dopants were added to the base PBZT composition. The niobium dopant concentrations were 0.5, 1, 2, and 4 mol% and the lanthanum concentrations were 1, 2, 3, and 4 mole%. Based on tolerance factor considerations [8], it was assumed that the Nb^{5+} ion is a 100% B-site substitution in the perovskite structure and La^{3+} is 50% A-site and 50% B-site.

Microstructural characterization was performed on the cross section of sintered pellets (fractured and/or polished surfaces) using scanning electron microscopy (SEM). To measure dielectric properties, sintered pellets were ground and polished to achieve flat and parallel surfaces onto which palladium-gold electrodes were sputtered. The capacitance and dielectric loss of each sample were measured as a function of DC bias, temperature, and frequency using an integrated, computer-controlled system. A schematic of the setup is shown in Fig. 1. Electric field from 0 to 20 kV/cm was applied to the sample using a high voltage power supply (Kepco Model BOP 1000M). During the measurement, a blocking circuit, was used to protect the LCR meter (Hewlett-Packard 4284A) from the DC bias voltage. The capacitance of the high voltage blocking capacitors was much larger ($>$20 times) than the samples for accurate measurements. The current limiting resistors and Zener diodes provide additional protection in the event of a catastrophic failure of the sample. The temperature of interest was the typical X7R range (−55 to 125°C) [9].

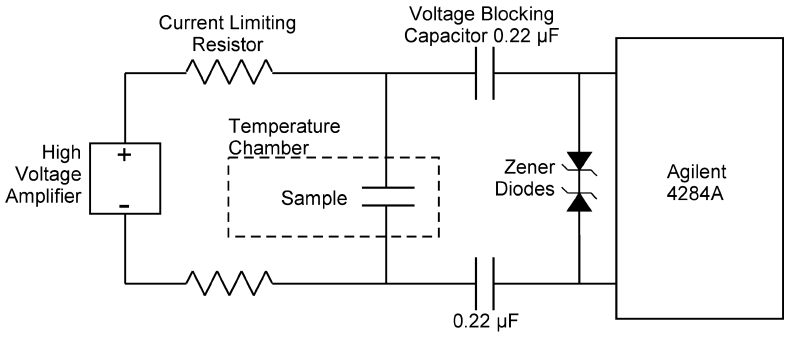

Fig. 1. A schematic of the blocking circuit used for the DC bias measurement. Both the high voltage amplifier and the LCR meter were controlled by a computer through a GPIB interface.

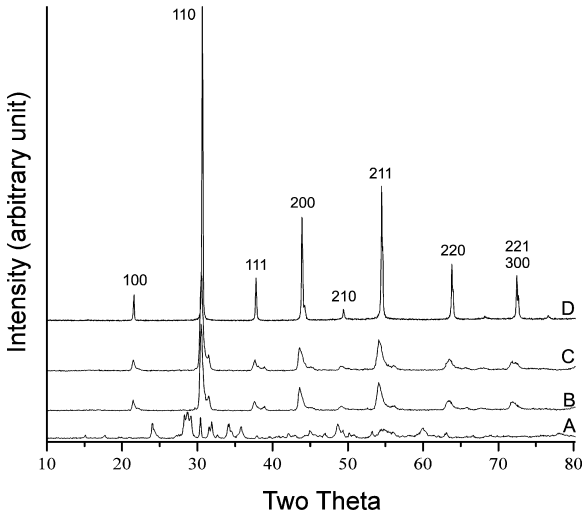

Fig. 2. XRD patterns showing the phase evolution during processing (A) attrition milled precursor powders, (B) calcined powder, (C) attrition milled calcined powder, and (D) sintered pellet.

Base PBZT Composition

Processing and Microstructure

XRD pattern of the initial samples showed that within the limits of detection they were single phase (Fig. 2). However, SEM micrographs of the polished surface of a sintered pellet showed that there was a small amount of ZrO_2 second phase (Fig. 3(a)). The cause of the second phase was believed to be the relatively large starting ZrO_2 particle size, which resulted in an incomplete solid state reaction during calcination. To reduce the particle size, as-received ZrO_2 powder was attrition-milled at 30 vol% solids loading prior to being batched with other raw powders. The particle size distribution of the attrition-milled powder was compared to the as-received powder in Fig. 4. The main difference between the powders was the percentage of particles that are below 1 μm. Subsequently, almost all of the ZrO_2 second phase was eliminated (Fig. 3(b)).

Dielectric Properties

According to Jaffe et al. [10], the base composition $(Pb_{0.65}Ba_{0.35})(Zr_{0.70}Ti_{0.30})O_3$ is a paraelectric phase at room temperature. Nevertheless, our dielectric results indicated that it is likely a relaxor with pseudo-cubic structure. It exhibited a very diffuse phase transition and the typical relaxor characteristics such as frequency dispersion, as shown in Fig. 5(a). Its dielectric constant is approximately 6000 at room temperature and remained almost constant under electric field as high as 20 kV/cm, as shown in Fig. 5(b) and (c).

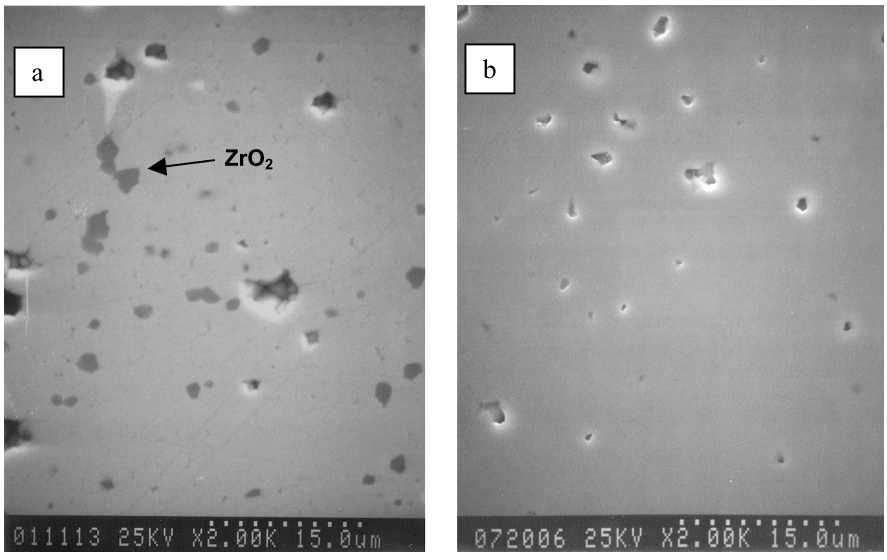

Fig. 3. SEM micrograph of the polished surface of a sintered pellet (a) using as received ZrO_2 powder as a precursor and (b) using attrition-milled ZrO_2 powder as a precursor.

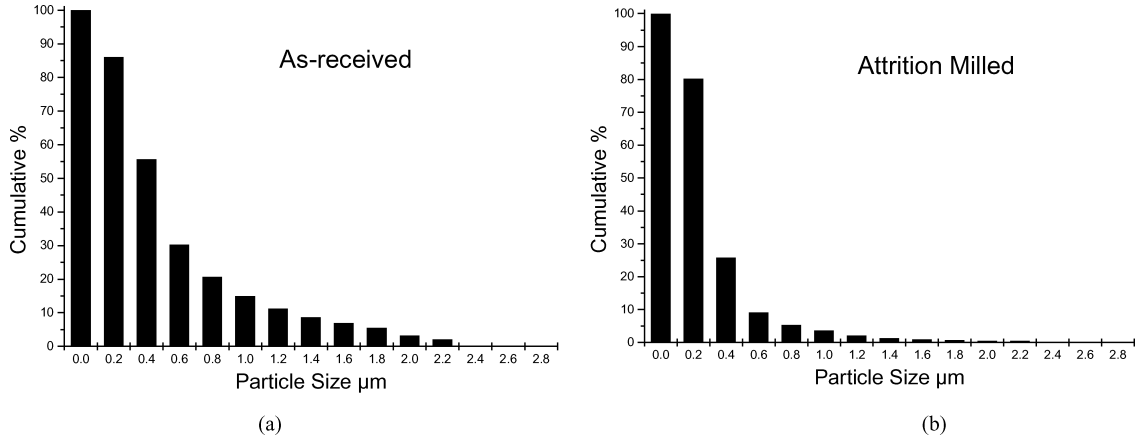

(a) (b)

Fig. 4. Particle size analysis of ZrO_2 powder (a) as-received and (b) attrition milled for 2 hours.

Dopant-Modified PBZT Compositions

Microstructure

The fracture surfaces of several samples are shown in Fig. 6. Most of the samples had a grain size of 2–3 μm, similar to that of the base PBZT. The exception was the 1% Nb-doped PBZT. The large grain size ($\sim$10 μm) and pores trapped within grains of the 1% Nb samples suggest rapid grain growth during sintering. To verify this observation, two more batches of 1% Nb PBZT was made and characterized. Both exhibited the same microstructure and dielectric properties. At present, it is not clear how Nb addition facilitates such abnormal grain growth, although similar behavior (initial increase in grain size at low dopant concentration and then decrease at higher concentrations) had been observed in $BaTiO_3$ with Nb dopant [11]. Nevertheless, it is not clear how the Nb content affects the sintering behavior in the PBZT system and the mechanism will be the subject of a future study.

Effects of Niobium Addition

The capacitance versus temperature (CvsT) plots of Nb-doped samples are shown in Fig. 7. All compositions exhibited diffuse phase transition and frequency dispersion. The temperature of the maximum dielectric constant (T_{max}) decreases with increasing Nb content with a rate of approximately 8.3°C per 1% Nb addition.

To better illustrate the effects of DC bias and temperature on dielectric constant (at 1 kHz) simultaneously, the data is shown as 3-D surface plots in Fig. 8. With the exception of the 1% Nb PBZT, the dielectric constant decreases slightly with increasing Nb content. Nevertheless, even with 4% Nb addition, the maximum dielectric constant is a respectable 4600. All of the Nb-doped samples appeared to have similar voltage/electric field stability as the original PBZT.

The 1% Nb PBZT exhibited a room temperature dielectric constant of 7400 at 1 kHz, a 20% improvement over the un-doped PBZT. As the 0.5% and 2% Nb samples did not show similar improvement, the high dielectric constant of 1% Nb samples was attributed to the large grain size. It has been reported that the dielectric constant of lead magnesium niobate-lead titanate (PMN-PT) relaxors increases with increasing grain size [12, 13]. In these references, the existence of a low dielectric constant grain boundary phase was used to explain and to quantify the observed grain size dependency. In the next section, we conducted a study on the effects of grain size on dielectric properties in Nb-doped PBZT relaxors to confirm this observation.

Effects of Lanthanum Addition

The interactions among dielectric constant, temperature, and applied electric field of La-doped PBZTs are illustrated in Fig. 9. It appears that La addition has a strong influence on both the magnitude of the dielectric constant and T_{max}, especially when the La content is >1%. The T_{max} decreases at a rate of 16.1°C per 1% La addition, about twice as fast as Nb addition. There

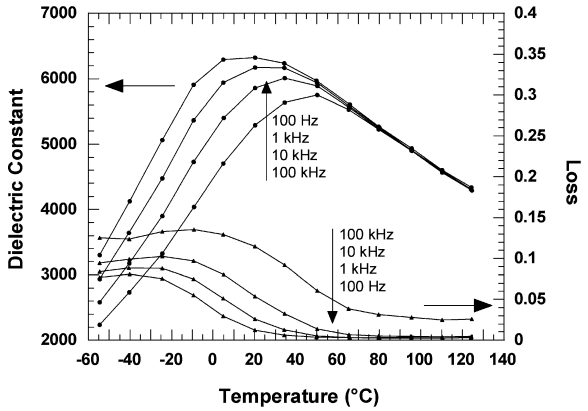

(a)

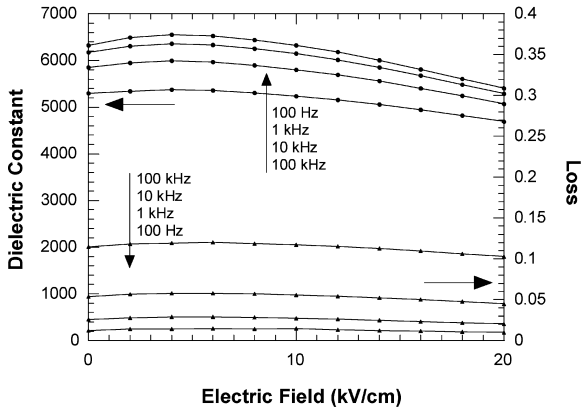

(b)

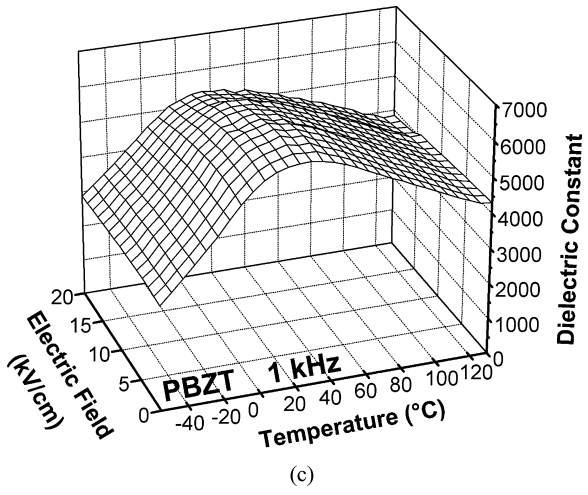

(c)

Fig. 5. The dielectric properties of the PBZT base composition showing (a) typical relaxor behavior measured low field (1 volt oscillation), (b) a stable voltage dependence at room temperature, and (c) dielectric constant plotted as a function of temperature and DC bias.

is a slight improvement in the temperature dependence and voltage stability of dielectric constant.

Effects of Grain Size on Dielectric Properties

Processing and Microstructure

As mentioned in the previous section, we planned to examine the correlation between grain size and dielectric properties in PBZT relaxors. The processing of PBZT modified with 0.5, 1, 2, and 3 mole% Nb_2O_5 was the same as described in the Experimental Procedure. Ceramic pellets were sintered at 1200, 1280, and 1330°C and the dwell time was 1, 2, and 3 hours for each of the sintering temperatures. The grain size was determined by the linear intercept method using scanning electron microscopy (SEM) micrographs of polished and etched sample surfaces. These sintering conditions produced samples with a range of grain size, which was summarized in Table 1. It appeared that 0.5 and 1% Nb samples had the largest grain size of all Nb concentrations. The rapid grain growth in 0.5 and 1% Nb samples was evidenced by the trapped pores along grain boundaries and within grains (similar to Fig. 6). We also observed a large scattering in the grain size of 0.5% Nb samples. It appeared that 0.5% Nb is at the threshold of the grain growth mechanism so that even slight composition inhomogeneity leads to large variations of microstructure and dielectric properties.

Dielectric Properties

Figure 10 shows the correlation between grain size and the dielectric maximum (K_{max}) for all the compositions. Note that, to have a reasonable comparison, the dielectric constant values have been adjusted for their respective porosity (V_2) using the following equation [14]:

$$K^* = K(1 + V_2/2)/(1 - V_2) \tag{1}$$

where K^* is the adjusted dielectric constant and K is the measured value. The porosity values were obtained by comparing the measured Archimedean density and the theoretical density, which was assumed to be 7.30 g/cm^3. The porosity ranges from 0.5 to 7.0 vol% with typical values between 1 and 3 vol%. The

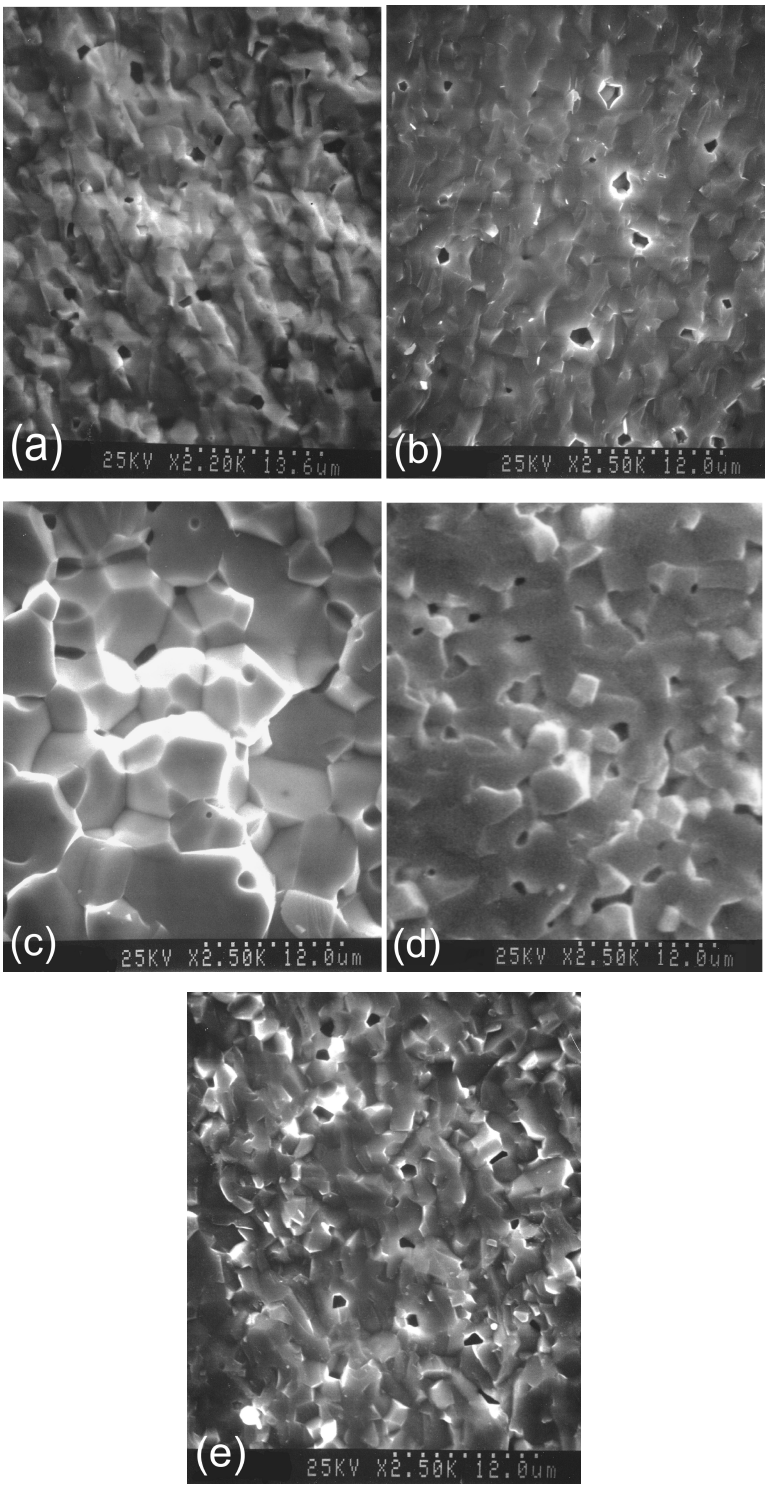

Fig. 6. SEM micrographs of the fracture surfaces of PBZTs with (a) 0%, (b) 0.5%, (c) 1%, (d) 2%, and (e) 4% Nb addition.

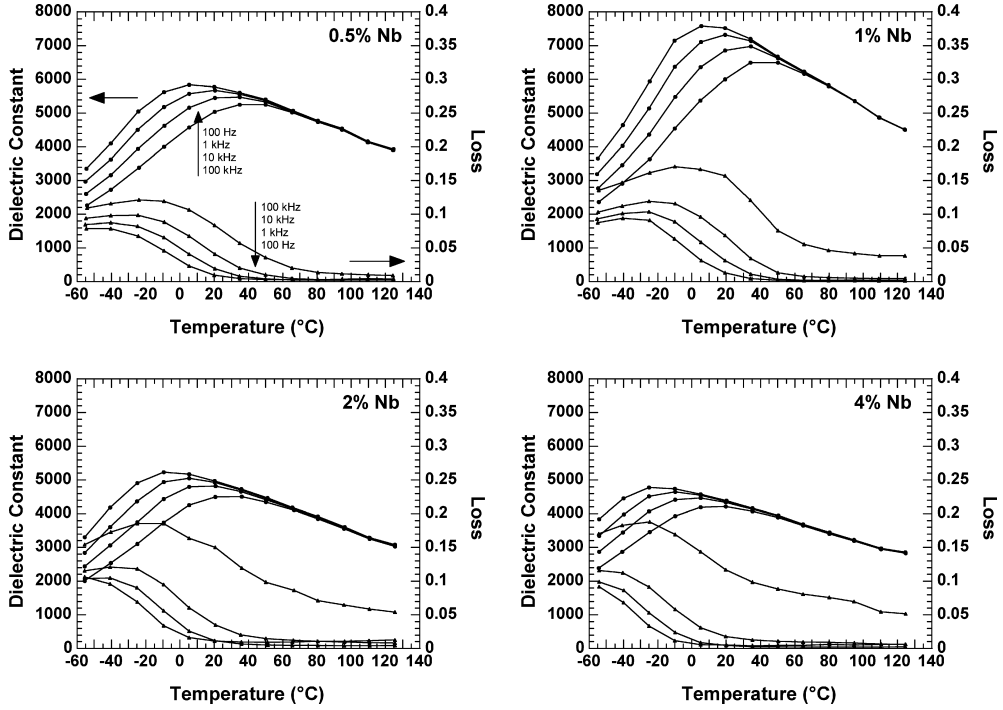

Fig. 7. The capacitance and loss versus temperature plots of Nb-doped samples.

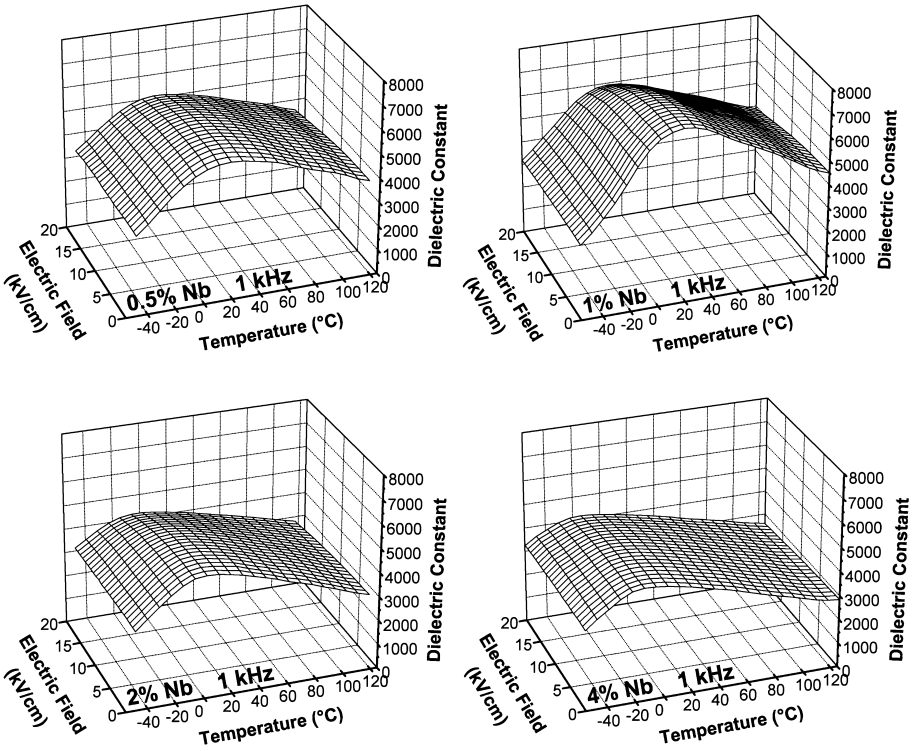

Fig. 8. 3-D surface plots of dielectric constant (1 kHz) as a function of temperature and DC bias for various Nb-doped PBZTs.

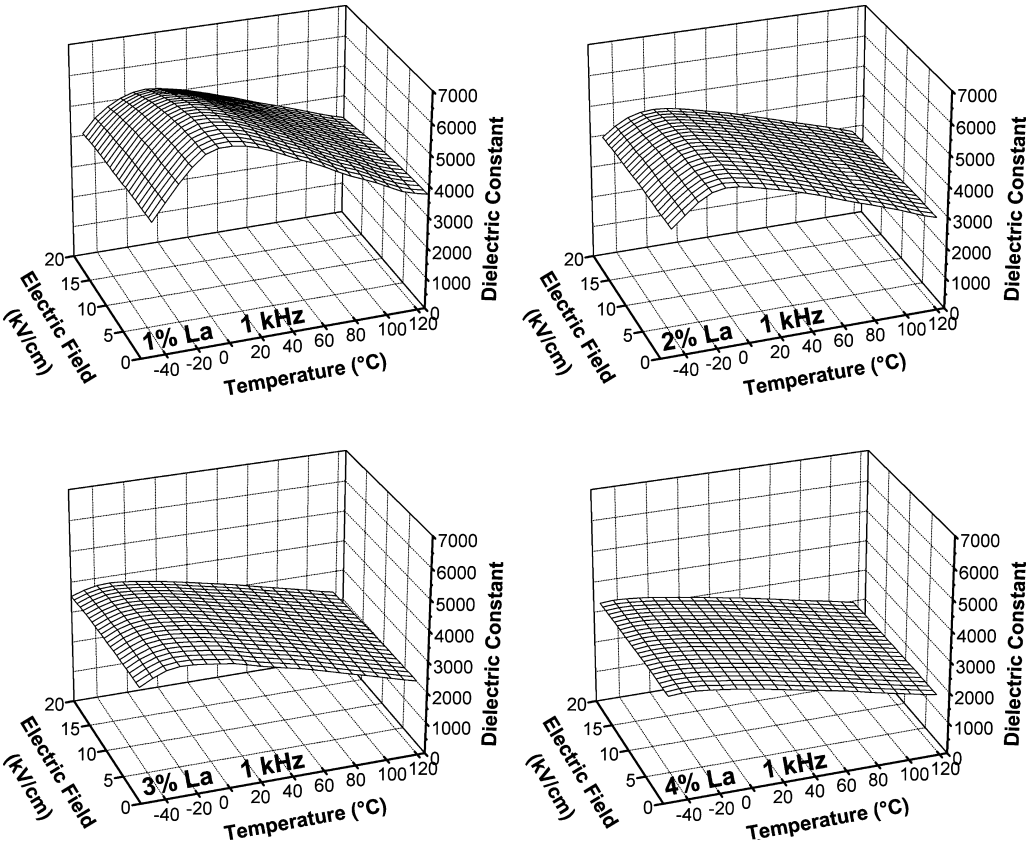

Fig. 9. 3-D surface plots of dielectric constant (1 kHz) as a function of temperature and DC bias for various La-doped PBZTs.

monotonic increase of K_{max} with increasing grain size is most evident in the group of 1% Nb samples. As mentioned in the previous section, the 0.5% Nb samples appeared to be at the threshold of rapid grain growth and consequently slight variations in compositional homogeneity and/or thermal history gave rise to large difference in microstructure. Consequently, the 0.5% Nb samples on which the dielectric properties were taken may not have the same microstructure as the polished sample from which grain size was measured. Finally, the size distribution of undoped samples is too narrow to draw any significant correlation and the 3% Nb addition has apparently adversely affected the dielectric properties.

Figure 11 shows the dielectric constant versus temperature (CvsT) plots of 1% Nb samples with three different grain sizes. It appeared that the temperature of dielectric maxima, T_{max}, was not

Table 1. A summary of the grain size produced at various sintering conditions (unit: μm).

Concentration of Nb (mole%)	1200°C			1280°C			1330°C		
	1 hr	2 hrs	3 hrs	1 hr	2 hrs	3 hrs	1 hr	2 hrs	3 hrs
0	2.2 ± 0.3	2.6 ± 0.3	2.0 ± 0.5	3.8 ± 0.4	3.4 ± 0.5	4.2 ± 0.6	3.2 ± 0.5	4.2 ± 0.7	4.4 ± 0.5
0.5	1.9 ± 0.3	4.8 ± 0.6	2.2 ± 0.4	10.7 ± 1.6	7.1 ± 0.9	12.7 ± 2.5	8.8 ± 1.5	8.5 ± 0.9	6.6 ± 1.2
1.0	3.9 ± 0.7	5.9 ± 0.7	7.6 ± 1.2	9.5 ± 1.8	9.4 ± 2.0	11.3 ± 1.6	11.7 ± 1.8	13.0 ± 2.5	11.7 ± 2.3
2.0	2.9 ± 0.6	3.1 ± 0.4	3.6 ± 0.4	4.5 ± 0.7	5.7 ± 0.9	7.5 ± 1.7	6.2 ± 0.8	7.9 ± 0.8	8.0 ± 1.3
3.0	2.0 ± 0.2	2.5 ± 0.4	2.7 ± 0.4	2.8 ± 0.4	4.1 ± 0.6	4.8 ± 1.1	6.0 ± 0.6	5.0 ± 0.6	7.0 ± 0.7

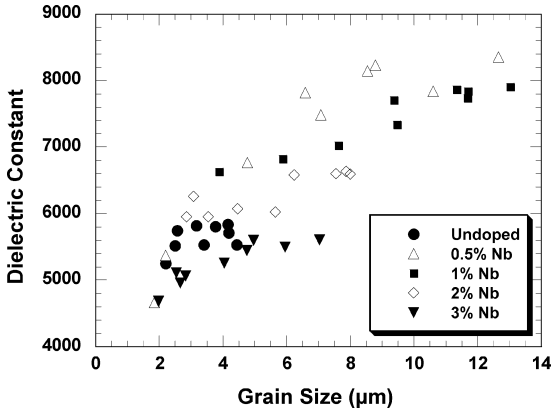

Fig. 10. The dielectric constant is plotted as a function of grain size for various Nb-doped PBZTs.

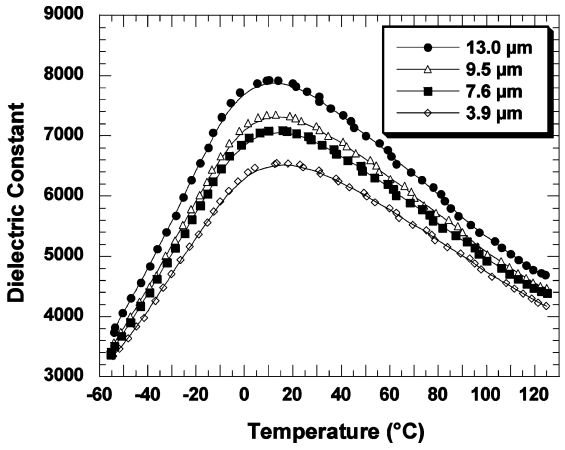

Fig. 11. Dielectric constant versus temperature plot of 1% Nb-doped PBZTs with various grain sizes (at 1 kHz).

sensitive to the change of grain size. This is consistent with the observation made by Randall et al. [12] on $Pb(Mg_{1/3}Nb_{2/3})O_3$:$PbTiO_3$ ceramics but is contrary to the observation on a similar PBZT composition by Sato et al. [15]. The reason for the discrepancy is not clear.

The application of a DC bias decreased T_{max}, as shown in Fig. 12. The decrease is approximately 8–10°C under a 20 kV/cm electric field for all compositions. Grain size did not change the amount of T_{max} shift. In addition, samples of various grain sizes showed the same percentage of K_{max} decrease under DC bias.

Influence of DC Bias on PBZTs

We believe that the remarkable dielectric stability under dc bias is a result of the order/disorder structure of

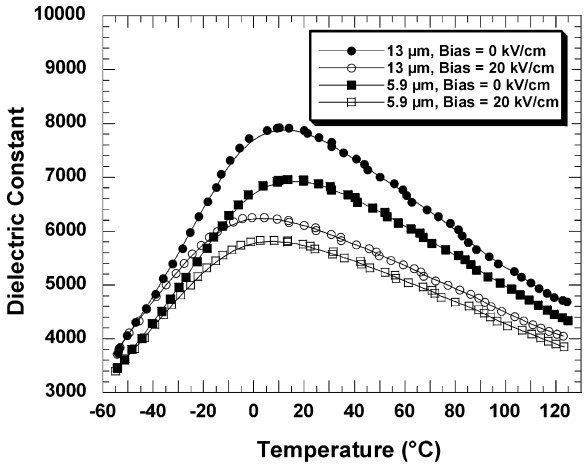

Fig. 12. Dielectric constant versus temperature behavior of 1% Nb-doped PBZTs under 0 and 20 kV/cm DC bias (at 1 kHz). Samples of two different grain sizes are shown.

relaxors from which microscopic composition inhomogeneities responded differently to the applied electric field. Similar stability in lead lanthanum zirconate titanate (PLZT) relaxors has been observed by Maher [16].

For normal ferroelectrics, the dielectric constant above the paraelectric-ferroelectric transition temperature can be described by the Curie-Weiss Law $K = 1+C/(T-T_0)$, where K is relative dielectric constant, C is the Curie constant, and T_0 is the Curie temperature. Note that the Curie constant C has the unit of temperature, indicative of the width of the phase transition peak. For relaxor ferroelectrics, however, the temperature dependence of dielectric constant is better described by a quadratic equation derived by Smolenskii [17]:

$$\frac{1}{K} = \frac{1}{K_{max}} + \frac{(T - T_{max})^2}{2K_{max}\delta^2} \qquad (2)$$

where K_{max} is the maximum dielectric constant, T_{max} is the temperature corresponds to maximum dielectric constant, and δ is the diffuseness coefficient. Although δ is not the same as the Curie constant C in the Curie-Weiss Law, one can observe the similarity of the two equations and therefore deduce that δ represents the "effective width" of the dielectric peak. The diffuseness coefficient δ can be determined from the slope of $1/K$ versus $(T - T_{max})^2$ plot. In the following discussion, all δ values were based on 1 kHz data.

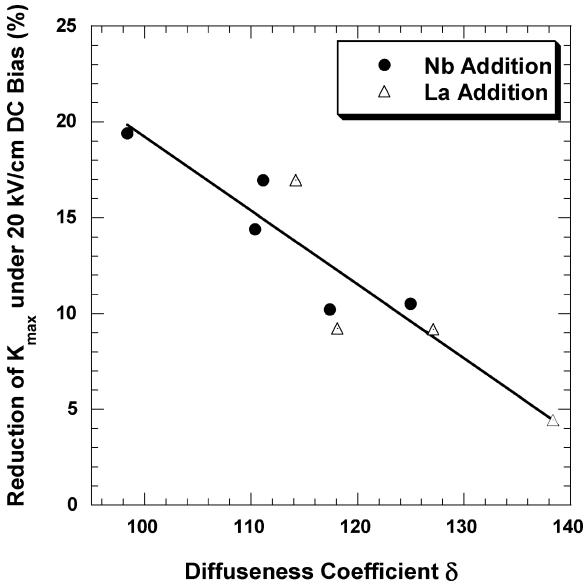

Fig. 13. A linear relation between the "diffuseness" and the dielectric stability under DC bias of PBZT relaxors is observed.

In Fig. 13, the reduction of $K_{\max}$ under 20kV/cm DC bias (compared to bias-free condition) is plotted against the diffuseness coefficient δ for all of the modified samples. Regardless of the type of dopant, a linear relation is observed—the larger the diffuseness coefficient, the more stable a material is under DC bias. It is apparent that a large diffuseness coefficient is due to a broad distribution of composition inhomogeneities in the relaxor material. The compositional variation leads to a widely distributed ferroelectric response under applied electric field and hence the voltage stability.

Conclusion

The effects of niobium oxide, lanthanum oxide, and grain size on the dielectric behavior of PBZT were evaluated in this study. Among all the compositions, the 1% Nb-doped PBZT exhibited a maximum dielectric constant (1 kHz) of 7400, an improvement of 20% over the un-modified PBZT. The results of the subsequent grain size study suggested that this improvement was a result of the large grain size in 1% Nb-doped PBZT, although the cause of abnormal grain growth at 1% Nb concentration is not clear. In general, the dielectric constant of Nb-doped PBZTs increases monotonically with increasing grain size, but decreases with increasing Nb concentration (except 1%). The La addition showed a large decrease of dielectric constant with increasing La content and hence is not considered a viable dopant. Neither dopants had a strong influence on the voltage stability of PBZTs. We also demonstrated that there is a linear relation between the diffuseness coefficient and the voltage stability, and therefore established the foundation for future composition engineering of the PBZT relaxors.

The dopant study and grain size study results suggests that an "optimized" PBZT with dielectric constant >7500 would have grain size >10 microns. Although such large grain size is not preferred for today's surface mount capacitors, we believe it would be suitable for the U.S. Navy's applications where the high voltage requirement ($\geq$4160V) and hence the thick dielectric layers would ensure a uniform electric field distribution.

References

1. G.R. Love, *J. Am. Ceram. Soc.*, **73**(2), 323 (1990).
2. W. Huebner, S.C. Zhang, M. Pennell, and X.M. Ding, in *Proceedings of the 8th US-Japan Seminar on Dielectric and Piezoelectric Ceramics* (Plymouth, MA, USA, 1997).
3. E. Moreira, J. de Mello, J. Povoa, D. Garcia, and J. Eiras, in *1996 IEEE Ultrasonics Symposium* (1996), Vol. 1, p. 527.
4. Z. Ujma, M. Adamczyk, and J. Handerek, *J. Eu. Ceram. Soc.*, **18**, 2201 (1998).
5. O. Furukawa, H. Kanai, and Y. Yamashita, *Jpn. J. Appl. Phys.*, **32**, 1708 (1993).
6. H. Kanai, O. Furukawa, H. Abe, and Y. Yamashita, *J. Am. Ceram. Soc.*, **77**, 2620 (1994).
7. A.J. Moulson and J.M. Herbert, in *Electroceramics: Materials, Properties, Applications* (Chapman & Hall, New York, 1990), p. 280.
8. H.D. Megaw, *Ferroelectricity in Crystals* (Methuen, London, 1957).
9. Electronic Industries Association Standard EIA-198.
10. B. Jaffe, W.R. Cook, Jr., and H. Jaffe, *Piezoelectric Ceramics* (Academic Press, 1971), p. 151.
11. M.N. Rahaman and R. Manalert, *J. Er. Ceram. Soc.*, **18**, 1063 (1998).
12. C.A. Randall, A.D. Hilton, D.J. Barber, and T.R. Shrout, *J. Mater. Res.*, **8**(4), p. 880 (1993).
13. P. Papet, J.P. Dougherty, and T.R. Shrout, *J. Mater. Res.*, **5**(12), 2902 (1990).
14. D.A. Payne and L.E. Cross, in *Ceramic Microstructures '76* (Westview Press, Boulder, Colorado, 1977), p. 584.
15. Y. Sato, H. Kanai, and Y. Yamoshita, *Jpn. J. Appl. Phys.*, **33**, 1380 (1994).
16. G.H. Maher, in *Proceedings of the 33rd IEEE Electronic Components Conference* (Orlando, Florida, 1983), p. 173.
17. G.A. Smolenskii, *J. Phys. Soc. Jpn.*, **28**(Suppl.), 26 (1970).